The Smoluchowski coagulation equations with continuous injection

1999 J. Phys. A: Math. Gen. 32 7745

(http://iopscience.iop.org/0305-4470/32/44/311)

J. Phys. A: Math. Gen. **32** (1999) 7745–7763. Printed in the UK PII: S0305-4470(99)05485-2

The Smoluchowski coagulation equations with continuous injection

Susan C Davies, John R King† and Jonathan A D Wattis†

Division of Theoretical Mechanics, School of Mathematical Sciences, University of Nottingham, University Park, Nottingham NG7 2RD, UK

E-mail: John.King@nottingham.ac.uk and Jonathan.Wattis@nottingham.ac.uk

Received 25 June 1999

Abstract. We study a system of equations which models the formation of clusters by coagulation, with particles of unit size being injected at a time-dependent rate. We observe that the criteria under which gelation occurs are the same as for the constant mass and constant monomer cases, which have been studied previously. We identify a variety of types of behaviour in the large-time limit, depending on the coagulation kernel and on the rate at which monomer is introduced into the system. The results are obtained by means of exact (generating function) techniques, matched asymptotic expansions and numerical simulations.

1. Introduction

We examine the Smoluchowski coagulation equations [20] with monomers being injected into the system at a rate $Q(t+t_0)^\omega$, so that the usual system generalizes to

$$\dot{c}_1 = Q(t+t_0)^\omega - \sum_{k=1}^{\infty} a_{k,1}c_k c_1 \tag{1.1}$$

$$\dot{c}_j = \tfrac{1}{2}\sum_{k=1}^{j-1} a_{k,j-k}c_k c_{j-k} - \sum_{k=1}^{\infty} a_{k,j}c_k c_j \qquad j \geqslant 2 \tag{1.2}$$

where $c_j(t)$ is the concentration of clusters of size j at time t, and the coagulation kernel $a_{k,j}$ specifies the rate at which clusters of sizes j and k coalesce. In the analysis that follows

$$a_{k,j} = \tfrac{1}{2}(j^\alpha k^\beta + j^\beta k^\alpha) \tag{1.3}$$

will be adopted. The constant Q can, without loss of generality, be scaled to unity, which henceforth we do. The moments of the distribution are defined by

$$M_p(t) = \sum_{k=1}^{\infty} k^p c_k(t) \qquad p = 0, 1, 2, \ldots. \tag{1.4}$$

A rigorous foundation for the study of the Smoluchowski coagulation equations has been provided by Ball and Carr [1], the existence and uniqueness of solutions being proved for aggregation kernels of the form $a_{j,k} = j^\alpha + k^\alpha$ and $a_{j,k} = (jk)^\alpha$. In the latter case, it is shown that gelation (mass loss) occurs if $\alpha > \frac{1}{2}$ and does so instantaneously if $\alpha > 1$. These results

† Authors to whom correspondence should be addressed.

0305-4470/99/447745+19$30.00

were extended to more general kernels by Carr and da Costa [2], who proved that instantaneous gelation occurs for any coefficients satisfying $j^\beta + k^\beta < a_{j,k} < (jk)^\alpha$ with $\alpha > \beta > 1$. Though these papers consider only the constant mass formulation of the problem, similar results hold for the problem in which mass is continuously added to the system.

The physical applications of this current work include the modelling of phase transitions in which the monomer is released at a time-dependent rate, for example, due to the decay of a precursor chemical, as occurs in cement hydration [21]. This method of releasing monomer into the coagulating system is in contrast to both (i) the constant monomer case, which models the pool chemical approximation where a supply of monomer is assumed to act in such a way as to maintain some artificially fixed concentration; and with (ii) the constant mass case, in which monodisperse initial conditions are typically assumed, so that at $t = 0$, the total mass of the system is instantaneously present in monomeric form and undergoes coagulation as time progresses. The Smoluchowski coagulation equations are used in modelling aerosol kinetics [11]. During the injection of a stream of particles into a chamber, matter injected at the beginning may start undergoing coagulation before all the matter has been introduced to the chamber. Thus a detailed model of the process requires the study of a system in which the total mass may vary in time. The Smoluchowski coagulation dynamics are also fundamental to polymerization kinetics, for example in the formation of worm-like micelles [16] (also known as living polymers), as well as in biochemical applications where they can be used to model the clustering of red blood cells [17].

We note that others have considered modifications to the coagulation equations in which matter is added to or removed from the system: in particular, Lushnikov and Kulmala [15], Crump and Seinfeld [3], Hendriks [9], Kleet [12], Simons [18] and Singh and Rodgers [19]. A general form of the equations which allows the addition of clusters of any size j, at a rate $Q_j(t)$, and removal, at a rate $R_j c_j$, is

$$\begin{aligned} \dot{c}_1 &= Q_1(t) - R_1 c_1 - \sum_{k=1}^{\infty} a_{k,1} c_k c_1 \\ \dot{c}_j &= Q_j(t) - R_j c_j + \tfrac{1}{2} \sum_{k=1}^{j-1} a_{k,j-k} c_k c_{j-k} - \sum_{k=1}^{\infty} a_{k,j} c_k c_j \qquad j \geqslant 2. \end{aligned} \tag{1.5}$$

The particular case we study thus corresponds to $R_j = 0$, $Q_j = 0$ for $j \geqslant 2$ and $R_1 = 0$, $Q_1(t) = (t + t_0)^\omega$. Another commonly studied case is that of constant monomer concentration, which corresponds to $Q_1 = \sum_{k=1}^{\infty} a_{k,1} c_k c_1$, $Q_j = 0$ for $j \geqslant 2$, $R_j = 0$. White [22], Kleet [12] and Crump and Seinfeld [3] were concerned with the existence of steady-state solutions in systems which have both addition and removal of matter. Crump and Seinfeld show that a steady-state solution exists if $\sum_{k=1}^{\infty} k^\gamma Q_k(t) < \infty$ for all γ and $R_k > Rk^\lambda$ for some $R > 0$, $\lambda \geqslant 0$ and $a_{j,k} < a(jk)^{\nu+\lambda}$ for some $a, \nu > 0$. However, as we shall see, the explicit removal of material need not be necessary for steady-state behaviour to occur, since if the aggregation kernel has the right form then mass is lost from the system by gelation, by which we mean the formation of an infinitely large particle which is not accounted for in the $c_j(t)$ cluster distribution function [23].

Some values of the exponent ω lead to divergent masses, and these should be interpreted as being intermediate asymptotic results; others do not lead to divergences and thus have a wider range of validity. There are three ranges of ω which we need to treat separately, namely (a) $-1 < \omega$, (b) $-2 < \omega < -1$ and (c) $\omega < -2$. The system is naturally divided into these cases by their different asymptotic behaviour at large times, as will be illustrated in detail in section 3. We sometimes include a positive constant t_0 in Q_1 to avoid a singularity for $\omega < 0$. Our prime focus is on how the large-time behaviour depends on the nature of the injection rate

(as characterized by ω); the form of this behaviour does not depend on the value of t_0. We typically take $t_0 = 0.01$ in the numerical simulations of section 3 and $t_0 = 0$ in the analytical solutions of section 2. Clearly, if $\omega < -1$ then only a finite amount of mass is added to the system and there are thus similarities with the constant mass case studied earlier [5]. However, if $\omega > -1$ then as $t \to \infty$ the mass contained within the system becomes unbounded; consequently, a different large-time asymptotic behaviour is observed. In this case there are similarities with the more commonly studied constant monomer concentration scenario [5]. Depending on the parameters α, β (for which we assume $\alpha \geqslant \beta \geqslant 0$), there are four gelation regimes: those of no gelation ($\alpha + \beta < 1$), delayed gelation ($1 < \alpha + \beta, \alpha < 1$), instantaneous gelation ($1 < \alpha < 1 + \beta$) and complete gelation ($\alpha > 1 + \beta$). The constraints on α and β under which each of these occurs are the same as for the constant mass and constant monomer cases described in [5].

In section 2 exact results are obtained for the 'integrable' cases in which α and β equal zero or one. The asymptotic behaviour of cases (a)–(c) will be examined in detail in section 3, with numerical methods being used to substantiate the three different regimes.

2. Analytical results

The systems with α and β equal to zero or one will be studied in some detail by a generating function technique. When mass is continuously being injected into the system, exact solutions are difficult to establish, but some important properties of the cluster size distribution function can nevertheless be gained for each of these systems.

We define the generating function by

$$C(z,t) = \sum_{j=1}^{\infty} c_j(t)\mathrm{e}^{-jz}. \tag{2.1}$$

For this quantity the zeroth, first and second moments are given by

$$M_0(t) = C(0,t) \qquad M_1(t) = -\frac{\partial}{\partial z}C(z,t)|_{z=0} \qquad M_2(t) = \frac{\partial^2}{\partial z^2}C(z,t)|_{z=0}. \tag{2.2}$$

M_0 gives the total number of clusters in the system and M_1 the total mass within these clusters, while M_2 can be used to detect gelation and to measure the polydispersity of the cluster distribution (defined by M_2M_0/M_1^2).

Our primary concern in this paper is with the large-time asymptotics of the system. However, initial conditions need to be specified for the exact solutions and the numerical simulations and for simplicity we take

$$c_1(0) = \varrho_0 \qquad c_j(0) = 0 \qquad \text{for} \quad j \geqslant 2. \tag{2.3}$$

Throughout this section we set $t_0 = 0$ and we treat only the regime $\omega > -1$.

2.1. Case I: $\alpha = \beta = 0$

With $\alpha = \beta = 0$, the substitution of the generating function into (1.1), (1.2) yields

$$\frac{\partial C}{\partial t} = t^{\omega}\mathrm{e}^{-z} - M_0C + \frac{1}{2}C^2. \tag{2.4}$$

By setting $z = 0$ in each of (2.4) and its first two derivatives with respect to z, equations for the first three moments can be found, namely

$$\frac{\mathrm{d}M_0}{\mathrm{d}t} = t^{\omega} - \frac{1}{2}M_0^2 \qquad \frac{\mathrm{d}M_1}{\mathrm{d}t} = t^{\omega} \qquad \frac{\mathrm{d}M_2}{\mathrm{d}t} = t^{\omega} + M_1^2. \tag{2.5}$$

The mass M_1 is thus given, as expected, by

$$M_1(t) = \varrho_0 + \frac{t^{\omega+1}}{\omega+1} \qquad \omega > -1 \tag{2.6}$$

being the sum of the initial mass and the injected mass, and this implies

$$M_2(t) = \varrho_0 + \varrho_0^2 t + \frac{t^{\omega+1}}{\omega+1} + \frac{2\varrho_0 t^{\omega+2}}{(\omega+1)(\omega+2)} + \frac{t^{2\omega+3}}{(\omega+1)^2(2\omega+3)}. \tag{2.7}$$

This is bounded for finite t, implying that the system does not gelate.

The zeroth moment in (2.5) satisfies a Riccati equation and so can be determined exactly. Thus the number of clusters $M_0(t)$ is given by

$$M_0(t) = \sqrt{2}t^{\omega/2}\left(\frac{AI_{-\frac{\omega+1}{\omega+2}}(\sqrt{2}t^{(\omega+2)/2}/(\omega+2)) + I_{\frac{\omega+1}{\omega+2}}(\sqrt{2}t^{(\omega+2)/2}/(\omega+2))}{AI_{\frac{1}{\omega+2}}(\sqrt{2}t^{(\omega+2)/2}/(\omega+2)) + I_{-\frac{1}{\omega+2}}(\sqrt{2}t^{(\omega+2)/2}/(\omega+2))}\right) \tag{2.8}$$

where I_ν is a modified Bessel function and

$$A = \varrho_0\Gamma\left(\frac{1}{\omega+2}\right)\Big/ 2^{\frac{\omega+1}{\omega+2}}(\omega+2)^{\frac{\omega}{\omega+2}}\Gamma\left(\frac{\omega+1}{\omega+2}\right). \tag{2.9}$$

The solution takes a much more transparent form for $\omega = 0$, in which case

$$M_0(t) = \sqrt{2}\tanh\left(\frac{t}{\sqrt{2}} + \tanh^{-1}\left(\frac{\varrho_0}{\sqrt{2}}\right)\right). \tag{2.10}$$

A large-time expansion of (2.8) yields the limiting behaviour $M_0 \sim \sqrt{2}t^{\omega/2}$ as $t \to \infty$. For $\omega > 0$ the total number of clusters thus grows unboundedly as $t \to \infty$, though significantly more slowly than the mass (2.6); for $\omega < 0$ the number of clusters decreases for large time, due to the rate at which clusters combine exceeding the injection rate. The large-time behaviour of the polydispersity of the distribution is given by

$$\frac{M_2M_0}{M_1^2} \sim \frac{\sqrt{2}t^{(\omega+2)/2}}{2\omega+3} \qquad \text{as} \quad t \to \infty. \tag{2.11}$$

Solutions (2.8) for M_0 corresponding to the first few positive integer values of ω are plotted in figure 1.

2.2. Case II: $\alpha = 1$, $\beta = 0$

Substitution of the generating function (2.1) into (1.1), (1.2) produces

$$\frac{\partial C}{\partial t} = t^\omega \mathrm{e}^{-z} - \frac{1}{2}CM_1 + \frac{1}{2}\frac{\partial C}{\partial z}(M_0 - C). \tag{2.12}$$

The mass is again given by (2.6), while the zeroth and second moments satisfy

$$\frac{\mathrm{d}M_0}{\mathrm{d}t} = t^\omega - \frac{1}{2}M_0M_1 \qquad \frac{\mathrm{d}M_2}{\mathrm{d}t} = t^\omega + M_1M_2 \tag{2.13}$$

the first of which can be solved in the form

$$M_0(t) = \left(\varrho_0 + \int_0^t s^\omega \exp\left(\frac{1}{2}\left(\varrho_0 s + \frac{s^{\omega+2}}{(\omega+2)(\omega+1)}\right)\right)\mathrm{d}s\right) \times \exp\left(-\frac{1}{2}\left(\varrho_0 t + \frac{t^{\omega+2}}{(\omega+2)(\omega+1)}\right)\right) \tag{2.14}$$

whereby $M_0 \sim 2(\omega+1)/t$ as $t \to \infty$ for $\omega > -1$. The second moment is given by

$$M_2(t) = \exp\left(\varrho_0 t + \frac{t^{\omega+2}}{(\omega+2)(\omega+1)}\right)\left[\varrho_0 + \int_0^t s^\omega \exp\left(-\varrho_0 s - \frac{s^{\omega+2}}{(\omega+2)(\omega+1)}\right)\mathrm{d}s\right] \tag{2.15}$$

showing that the polydispersity grows extremely rapidly in the limit $t \to \infty$.

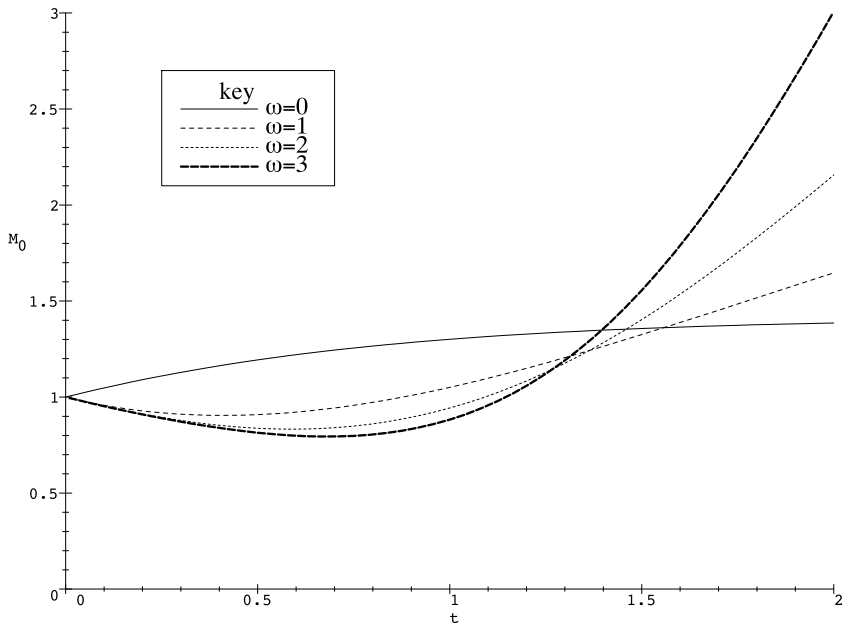

Figure 1. Plot of the zeroth moment with $\omega = 0, 1, 2, 3$ for $\alpha = \beta = 0$.

2.3. Case III: $\alpha = \beta = 1$

In this case gelation occurs within a finite time, after which (2.6) ceases to be valid due to mass being lost to the gel. The substitution of the generating function (2.1) into (1.1), (1.2) now leads to

$$\frac{\partial C}{\partial t} = t^{\omega}\mathrm{e}^{-z} + M_1\frac{\partial C}{\partial z} + \frac{1}{2}\left(\frac{\partial C}{\partial z}\right)^2. \tag{2.16}$$

Introducing $u = -\partial C/\partial z$ yields

$$\frac{\partial u}{\partial t} = t^{\omega}\mathrm{e}^{-z} + (M_1 - u)\frac{\partial u}{\partial z}. \tag{2.17}$$

Prior to the gelation time $t = t_g$, (2.6) holds, implying that the characteristic equations for (2.17) are

$$\frac{\mathrm{d}z}{\mathrm{d}t} = u - 1 - \frac{1}{\omega+1}t^{\omega+1} \qquad \frac{\mathrm{d}u}{\mathrm{d}t} = t^{\omega}\mathrm{e}^{-z}. \tag{2.18}$$

Gelation occurs when $\partial u/\partial z$ becomes unbounded at $z = 0$ (cf [5]). The gelation time can be obtained from the second moment—differentiating (2.17) with respect to z and setting $z = 0$ gives

$$\frac{\mathrm{d}M_2}{\mathrm{d}t} = t^{\omega} + M_2^2 \qquad \text{for} \quad t < t_g \tag{2.19}$$

which is a Riccati equation with solution

$$M_2(t) = t^{\omega/2}\left(\frac{AJ_{-\frac{\omega+1}{\omega+2}}(2t^{(\omega+2)/2}/(\omega+2)) + J_{\frac{\omega+1}{\omega+2}}(2t^{(\omega+2)/2}/(\omega+2))}{-AJ_{\frac{1}{\omega+2}}(2t^{(\omega+2)/2}/(\omega+2)) + J_{-\frac{1}{\omega+2}}(2t^{(\omega+2)/2}/(\omega+2))}\right) \tag{2.20}$$

where J_ν is a Bessel function and

$$A = \varrho_0\Gamma\left(\frac{1}{\omega+2}\right)\Big/(\omega+2)^{\frac{\omega}{\omega+2}}\Gamma\left(\frac{\omega+1}{\omega+2}\right). \tag{2.21}$$

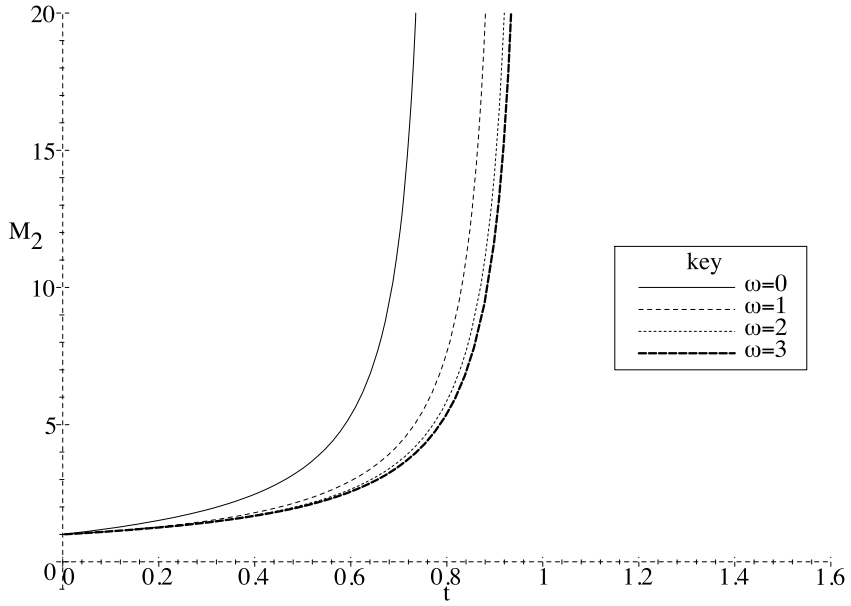

Figure 2. Plot of the second moment with $\omega = 0, 1, 2, 3$ for $\alpha = \beta = 1$ and $\varrho_0 = 1$.

The evolution of $M_2(t)$ for $\varrho_0 = 1$ and $\omega = 0, 1, 2, 3$ can be seen in figure 2, the gelation time (t_g) corresponding to where M_2 blows up. When $\omega = 0$, (2.19) is separable and it readily follows that

$$M_2(t) = \tan(t + \tan^{-1}\varrho_0) \qquad t_g = \tan^{-1}(1/\varrho_0). \tag{2.22}$$

The number of clusters $M_0(t)$ satisfies

$$\frac{\mathrm{d}M_0}{\mathrm{d}t} = t^{\omega} - \frac{1}{2}M_1^2 \tag{2.23}$$

so prior to gelation is given by

$$M_0(t) = \varrho_0 - \frac{1}{2}\varrho_0^2 t + \frac{t^{\omega+1}}{\omega+1} - \frac{\varrho_0 t^{\omega+2}}{(\omega+1)(\omega+2)} - \frac{t^{2\omega+3}}{2(\omega+1)^2(2\omega+3)}. \tag{2.24}$$

For $\alpha = \beta = 1$ the numerical approach outlined below leads to a value of $t_g \approx 0.7$ when $\varrho_0 = 1$, in fair agreement with the value $\pi/4$ predicted by (2.22) (given the delicacy of assessing gelation from a truncated system) and thus helps provide confidence in the numerical results. Figure 3(*a*) shows the dependence of the gelation time t_g on the injection exponent (ω) determined from (2.20) for both the cases $\varrho_0 = 1$ and $\varrho_0 = 0$. The former illustrates that when $\omega = 0$, the gelation time is $\pi/4$ and as ω increases, the gelation time asymptotes to the constant mass result of $t_g = 1$, which holds when the source term is absent [13]. The gelation time tends to zero as $\omega \to -1$. For the case in which there is initially no mass present in the system ($\varrho_0 = 0$) we have $t_g \sim (\omega + 1)$ as $\omega \to -1$ and $t_g \to 1$ with $\log t_g \sim 2\log(\omega)/\omega$ as $\omega \to \infty$. There is a maximum in the gelation time at $\omega = \frac{3}{2}$, where $t_g = 2$.

In figure 3(*b*) the mass at the gelation time is plotted against ω illustrating the expected results that for $\varrho_0 = 1$ in the limit $\omega \to \infty$ the system behaves as the constant mass case with $M_1(t_g) \to 1$, and that $M_1(t_g) \to \infty$ as $\omega \to -1$. For the case $\varrho_0 = 0$ we have $M_1(t_g) \sim 1/(\omega+1)$ as $\omega \to -1$ and $M_1(t_g) \sim \omega$ as $\omega \to \infty$. There is a minimum in the mass at gelation when $\omega = 0$, where $M_1(t_g) = \pi/2$.

Little analytical progress is possible for $t > t_g$.

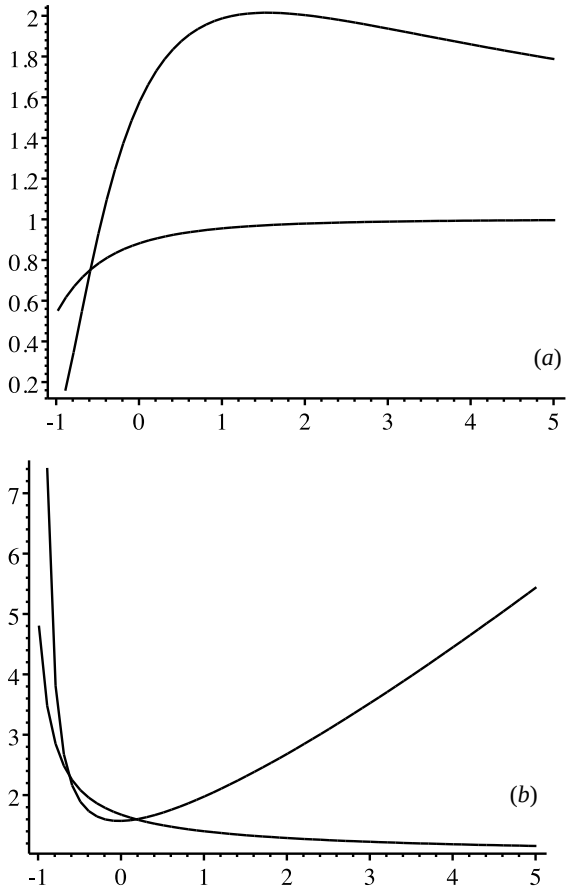

Figure 3. (*a*) The gelation time (t_g) against the injection exponent (ω): the upper curve corresponds to the case $\varrho_0 = 0$, and the lower to $\varrho_0 = 1$; (*b*) the mass at the gel point against ω: the curve which rises at larger ω corresponds to the case $\varrho_0 = 0$, the other curve being the case $\varrho_0 = 1$. All graphs correspond to $\alpha = \beta = 1$.

2.4. Steady-state solutions

In the gelating regime $\alpha + \beta > 1$, $|\alpha - \beta| < 1$ a steady-state solution exists for $\omega = 0$, the system losing mass through gelation at the same rate as it is acquired through injection. Writing $c_j(t) = g_j$ we have

$$\begin{aligned} 0 &= 1 - \tfrac{1}{2}\sum_{k=1}^{\infty}(k^\beta + k^\alpha)g_k g_1 \\ 0 &= \tfrac{1}{4}\sum_{k=1}^{j-1}(k^\alpha(j-k)^\beta + k^\beta(j-k)^\alpha)g_k g_{j-k} - \tfrac{1}{2}\sum_{k=1}^{\infty}(j^\alpha k^\beta + j^\beta k^\alpha)g_k g_j \qquad j \geqslant 2. \end{aligned} \tag{2.25}$$

For $\alpha = \beta$, this steady state can be constructed explicitly (using the generating function $D(z) = \sum_{k=1}^{\infty} k^\alpha g_k \mathrm{e}^{-kz}$), giving, in a similar fashion as in [5],

$$g_j = \frac{\sqrt{2}(2j)!\,j^{-\alpha}}{j!\,j!2^{2j}(2j-1)}. \tag{2.26}$$

Here we have $g_1 = 1/\sqrt{2}$, the solution thus being smaller than the constant monomer steady-state solution for $g_1 = 1$ by a factor $\sqrt{2}$.

3. Asymptotic and numerical results

3.1. Introduction

The methods of the previous section are of limited value for arbitrary α and β and in this section we instead focus directly on the large-time behaviour. In this limit, the distribution function often varies slowly with j for large j, in which case the leading-order asymptotic problem is given by the continuum limit, whereby the discrete equations are approximated by a continuous formulation of the problem. The large-time asymptotic results are split into three sections, dependent on the value of ω, namely (a) $-1 < \omega$, (b) $-2 < \omega < -1$ and (c) $\omega < -2$; the analysis involves an application of the method of matched asymptotic expansions. For non-gelating systems, each regime will comprise either one or two outer regions, in which to leading order the solution satisfies the continuum formulation whereby, writing $c_j(t) = c(x,t)$, we have

$$\frac{\partial c(x,t)}{\partial t} = \int_0^{x/2} c(y,t)[a(y,x-y)c(x-y,t) - a(y,x)c(x,t)]\,\mathrm{d}y - c(x,t)\int_{x/2}^{\infty} a(y,x)c(y,t)\,\mathrm{d}y \tag{3.1}$$

and an inner region $j = \mathrm{O}(1)$ in which the concentrations are governed by the discrete system. In gelating systems the 'inner' solution is valid for all j. For the initial conditions (2.3), we have

$$M_1(t) = \varrho_0 + \frac{1}{\omega+1}((t+t_0)^{\omega+1} - t_0^{\omega+1}) \qquad \omega \neq -1 \tag{3.2}$$

in non-gelating cases (and prior to gelation in cases that exhibit finite-time gelation).

Numerical results for each range of ω have been obtained [4] for each of the four gelation regimes, namely no, finite-time, instantaneous and complete gelation. A FORTRAN 77 program using the NAG routine D02NBF was used to solve the stiff system of ordinary differential equations which represent a truncated version of the coagulation equations, namely

$$\dot{c}_1(t) = (t+t_0)^{\omega} - \sum_{k=1}^{N-1} a_{k,1}c_k c_1 \tag{3.3}$$

$$\dot{c}_j(t) = \tfrac{1}{2}\sum_{k=1}^{j-1} a_{k,j-k}c_k c_{k-j} - \sum_{k=1}^{N-j} a_{k,j}c_k c_j \qquad j \geqslant 2. \tag{3.4}$$

In this truncation no cluster of size greater than N is allowed to form, with no mass being lost from the system. The maximum cluster size was taken to be $N = 400$ in all simulations, which is adequate in most cases, and we take $t_0 = 0.01$. A variety of gelation criteria were tested, the most robust and accurate was found to be taking gelation to have occurred if the concentration of the maximum cluster size exceeds 10^{-7}, this value being significantly larger than the numerical errors in the simulation, and the same order of magnitude as is expected for c_N at the gel point, namely $c_j = \mathrm{O}(j^{-(\alpha+\beta+1)/2})$. Gelation is thus detected numerically at a slightly earlier time than it in fact occurs, because of the truncation of the system at a finite cluster size. Numerical solutions nevertheless convincingly substantiate the asymptotic results, as illustrated below. Tests with $N = 200$ and 400 were carried out and little difference observed (an assessment of different numerical criteria for detecting the onset of gelation is given in [4]).

3.2. The case $\omega > -1$

The leading-order outer solution in non-gelating cases can be assumed to satisfy (3.1) and to take the form

$$c = t^{-p}h(\zeta) \qquad \zeta = x/t^q \qquad \text{with} \quad p - (\alpha + \beta + 1)q = 1 \tag{3.5}$$

where the values of p and q are specified by ensuring that the mass in the outer region is consistent with (3.2) in the large-time limit; thus

$$\int_0^\infty xc(x,t)\,\mathrm{d}x \sim \frac{t^{\omega+1}}{\omega+1} \qquad \text{as} \quad t \to \infty \tag{3.6}$$

(this holds for any t_0), which gives

$$p = \frac{\omega + 3 + (\alpha+\beta)(\omega+1)}{1-(\alpha+\beta)} \qquad q = \frac{\omega+2}{1-(\alpha+\beta)} \tag{3.7}$$

with

$$\int_0^\infty \zeta h(\zeta)\,\mathrm{d}\zeta = \frac{1}{\omega+1}. \tag{3.8}$$

Thus the outer solution as $t \to \infty$ is of the form

$$c \sim t^{-\frac{(\omega+3+(\alpha+\beta)(\omega+1))}{1-(\alpha+\beta)}} h(\zeta) \qquad \zeta = x/t^{\frac{\omega+2}{1-(\alpha+\beta)}}. \tag{3.9}$$

Figure 4 gives a plot of $\log(c_j t^p)$ against $\log(jt^{-q})$ for the case $\alpha = 0.3$, $\beta = 0.1$ (lying in the non-gelating regime $\alpha + \beta < 1$) with p and q given by (3.7); it can be seen that, at large

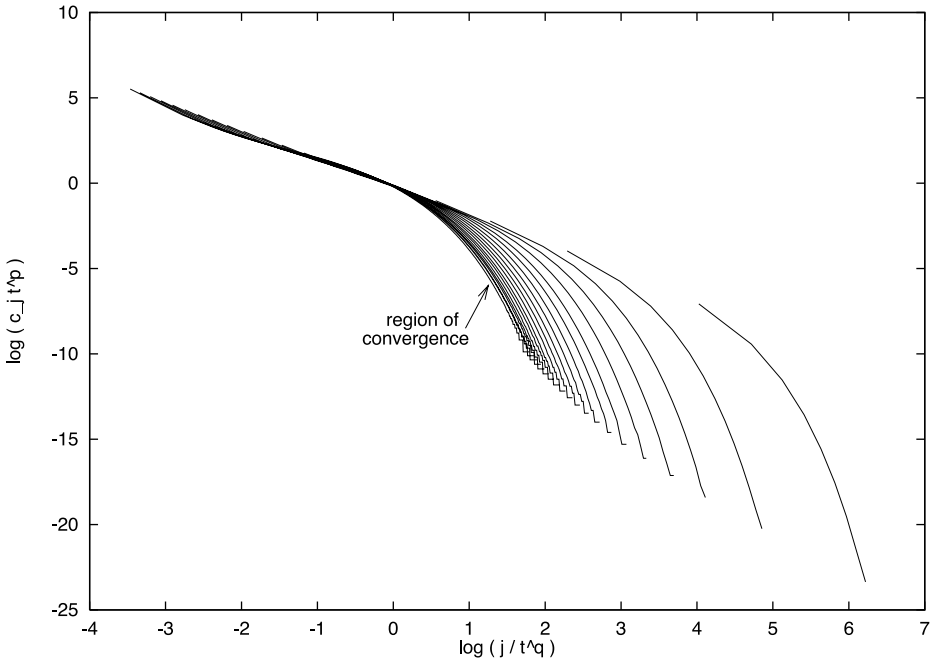

Figure 4. Plot of $\log(c_j t^p)$ against $\log(jt^{-q})$ for $\omega = -0.5$, $\alpha = 0.3$, $\beta = 0.1$, at times $t = 0.2$–4 in steps of 0.2, plotted in terms of the similarity variables in (3.9): i.e. (3.5) with $p = \frac{9}{2}$ and $q = \frac{5}{2}$. The lower ends of the curves move to the left as time increases. The results clearly illustrate convergence to the outer similarity solution.

times, the curves become almost indistinguishable. This indicates that the self-similar form is being approached, the limiting curve being given by the function $h(\zeta)$ in (3.9).

In the inner region $j = \mathrm{O}(1)$, a quasi-steady balance holds in (1.1), (1.2), with

$$c_j \sim t^{\omega/2} g_j \qquad t \to \infty \tag{3.10}$$

where the g_j are independent of time and of ω, being given by (2.25) (when substituted into the governing equations (1.1) and (1.2), (3.10) implies that the time derivatives are negligible in the large-time limit, the aggregation of smaller particles to form a j-cluster being balanced by the aggregation of j-clusters to form larger particles). Expression (3.10) can thus be regarded as a generalization of the steady-state solution which applies in the special case $\omega = 0$.

The matching between inner and outer solutions is as follows. We have for (2.25) that

$$g_j \sim A j^{-(\alpha+\beta+3)/2} \qquad \text{as} \quad j \to \infty \tag{3.11}$$

for some constant A; when $\alpha = \beta$, (2.26) gives $A = 1/\sqrt{2\pi}$. Because the outer limit of the inner solution is given by (3.11), we require that the inner limit of the outer solution satisfy

$$h(\zeta) \sim A\zeta^{-(\alpha+\beta+3)/2} \qquad \text{as} \quad \zeta \to 0^+ \tag{3.12}$$

and from matching between (3.11) and (3.12) we have

$$c_j \sim A t^{\omega/2} j^{-(\alpha+\beta+3)/2} = A t^{-\frac{\omega+3+(\omega+1)(\alpha+\beta)}{1-(\alpha+\beta)}} (j/t^{\frac{\omega+2}{1-(\alpha+\beta)}})^{-(\alpha+\beta+3)/2} \tag{3.13}$$

as required.

The convergence for large t to the postulated inner solution (3.10) can also be confirmed numerically (see [4]). In the gelating regime the solution (3.10) is uniformly valid for large times. This is illustrated in figure 5, which shows for $\alpha = 0.9$, $\beta = 0.5$ how the solution

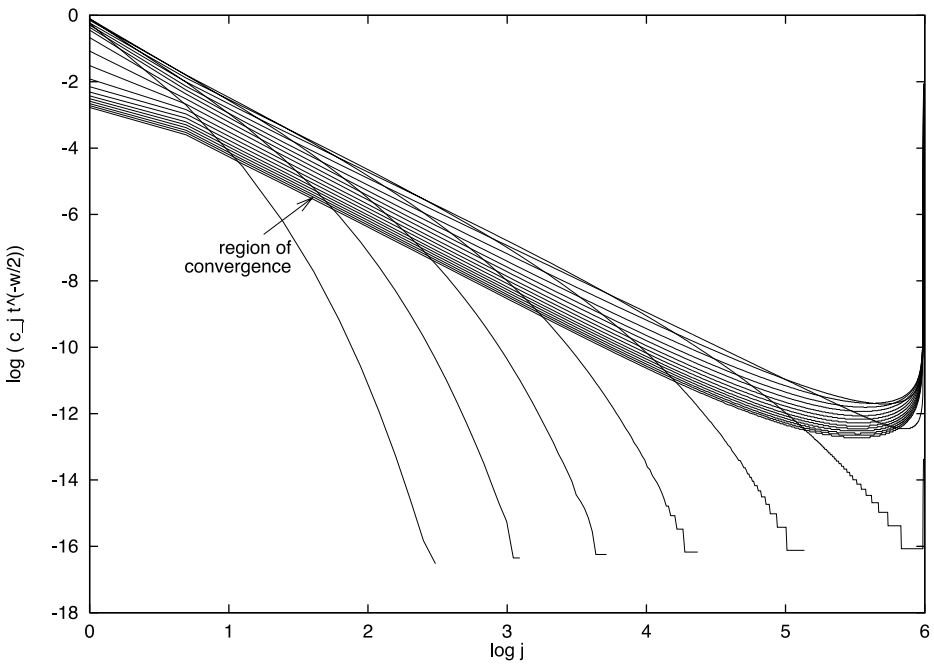

Figure 5. Plot of $\log(c_j t^{-\omega/2})$ against $\log j$ at times $t = 0.2$–4, in steps of 0.2, for $\omega = -0.5$ and $\alpha = 0.9$, $\beta = 0.5$. Effects due to truncation are evident for large j at the later times, but elsewhere convergence to (3.10) is exhibited.

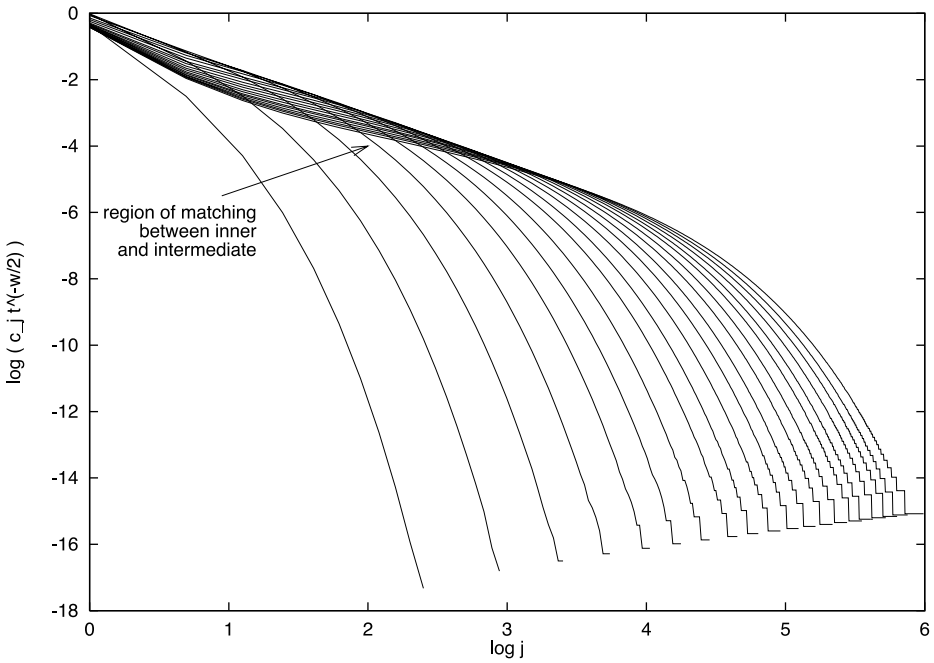

Figure 6. Plot of $\log(c_j t^{-\omega/2})$ against $\log j$ at times $t = 0.2$–4, in steps of 0.2, for $\omega = -1.5$ and $\alpha = 0.3$, $\beta = 0.1$, showing convergence to the inner (quasi-steady) solution.

converges for large time to a single curve, which on the log–log plot approaches a straight line with gradient -2.4 for large enough cluster sizes. This is in close agreement with (3.11), since $-(\alpha + \beta + 3)/2 = -2.2$.

For $\omega = -1$, the expression (3.10) again describes the inner region, but because (3.6) is replaced by

$$\int_0^\infty x c(x,t)\,\mathrm{d}x \sim \log t \qquad \text{as} \quad t \to \infty \tag{3.14}$$

the outer similarity solution takes the form

$$c \sim t^{-\frac{2}{1-(\alpha+\beta)}} \log^{-\frac{1+\alpha+\beta}{1-(\alpha+\beta)}} t h(\zeta) \qquad \zeta = x/t^{\frac{1}{1-(\alpha+\beta)}} \log^{\frac{1}{1-(\alpha+\beta)}} t \tag{3.15}$$

in place of (3.9).

3.3. The case $-2 < \omega < -1$

In this case there are three regions, inner, intermediate and outer. The leading-order inner solution is of the quasi-steady form (3.1), this being illustrated numerically in figure 6. The intermediate and outer solutions are given to leading order by similarity solutions of (3.10), which we write in the form

$$\text{intermediate} \qquad c = t^{-p} h(\zeta) \qquad \zeta = x/t^q \qquad \text{with} \quad p - (\alpha + \beta + 1)q = 1 \tag{3.16}$$

$$\text{outer} \qquad c = t^{-m} g(\eta) \qquad \eta = x/t^n \qquad \text{with} \quad m - (\alpha + \beta + 1)n = 1. \tag{3.17}$$

Since the inner solution is again of the quasi-steady form (3.10), matching requires, as before, that p and q in (3.16) be given by (3.7). This is demonstrated in figure 7, where results for $\omega = -1.5$, $\alpha = 0.3$ and $\beta = 0.1$ are displayed as a plot of $\log(c_j t^{-1.3/0.6})$ against

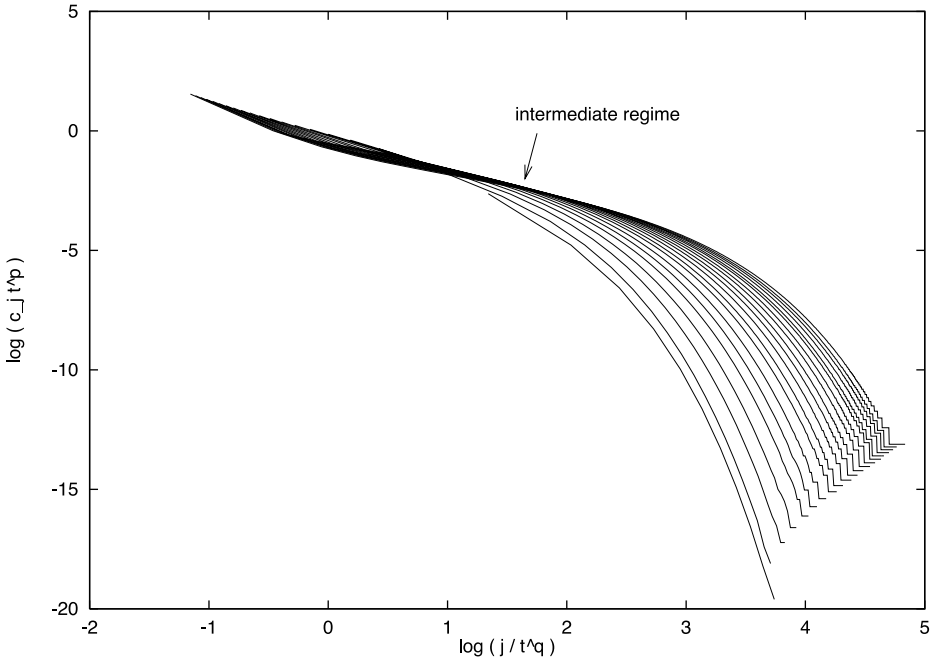

Figure 7. Plot of $\log(c_j t^p)$ against $\log(j/t^q)$ with $p = \frac{13}{6}$ and $q = \frac{5}{6}$ showing convergence of the intermediate solution at times $t = 0.2$–4, in steps of 0.2, for $\omega = -1.5$ and $\alpha = 0.3$, $\beta = 0.1$. Curves corresponding to later times are higher up and agree with the intermediate asymptotic result over a greater horizontal interval.

$\log(jt^{-0.5/0.6})$, the curves at later times approaching a single curve for intermediate cluster size.

The values of m and n in (3.17) for the outer solution are determined by requiring from (3.2) that

$$\int_0^\infty xc(x,t)\,\mathrm{d}x \sim \varrho_0 - \frac{1}{\omega+1}t_0^{\omega+1} \qquad \text{as} \quad t \to \infty \tag{3.18}$$

yielding (as in the constant mass case [5])

$$m = \frac{2}{1-(\alpha+\beta)} \qquad n = \frac{1}{1-(\alpha+\beta)} \tag{3.19}$$

with

$$\int_0^\infty \eta g(\eta)\,\mathrm{d}\eta = \rho_0 - \frac{1}{\omega+1}t_0^{\omega+1}. \tag{3.20}$$

We note that $n > q$, as required, for $\omega < -1$, $\alpha + \beta < 1$.

Figure 8 illustrates the outer asymptotic form

$$c(x,t) \sim t^{-\frac{2}{1-(\alpha+\beta)}} g(\eta) \qquad \eta = x/t^{\frac{1}{1-(\alpha+\beta)}} \qquad \text{as} \quad t \to \infty \qquad \eta = \mathrm{O}(1) \tag{3.21}$$

the curves there becoming superimposed for large-time and large cluster size. Matching the outer solution to the intermediate one gives

$$\begin{aligned} g(\eta) &\sim \frac{2\alpha\beta\eta^{-(\alpha+\beta+1)}}{(1-(\alpha+\beta))(\alpha+\beta)B(1-\alpha,1-\beta)} \qquad \text{as} \quad \eta \to 0^+ \\ h(\zeta) &\sim \frac{2\alpha\beta\zeta^{-(\alpha+\beta+1)}}{(1-(\alpha+\beta))(\alpha+\beta)B(1-\alpha,1-\beta)} \qquad \text{as} \quad \zeta \to +\infty \end{aligned} \tag{3.22}$$

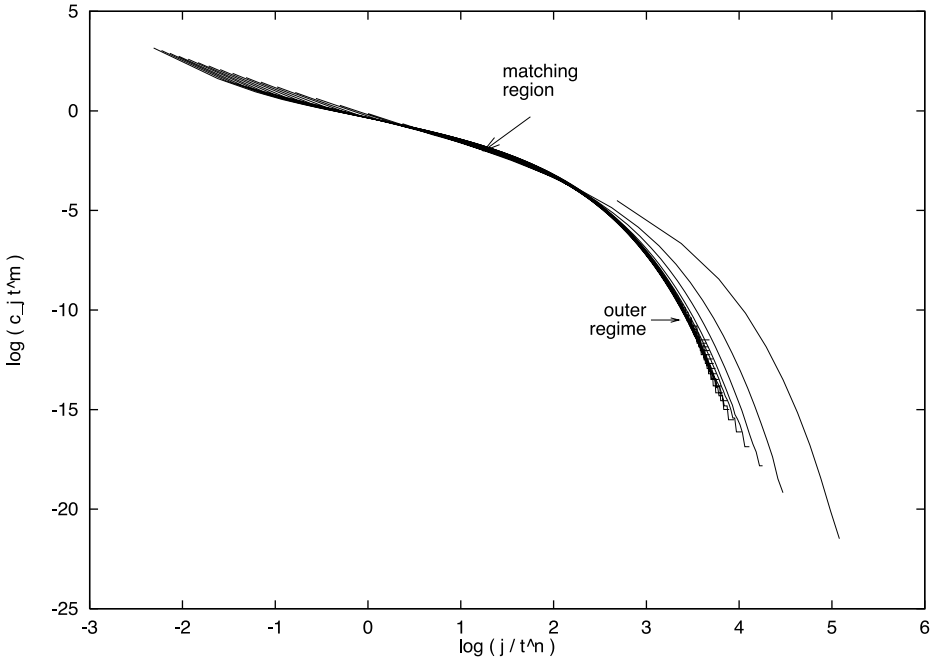

Figure 8. Plot of $\log(c_j t^m)$ against $\log(j/t^n)$ with $m = \frac{10}{6}$ and $n = \frac{5}{3}$ showing the outer solution at times $t = 0.2$–4, in steps of 0.2, for $\omega = -1.5$ and $\alpha = 0.3$, $\beta = 0.1$. As time increases the lowest portion of each curve moves to the left

the first of which follows from [5]; $h(\zeta)$ again satisfies (3.12) as the condition for matching with the inner solution. The result (3.22) can be compared with the numerics in figure 8 where, for intermediate j, a straight line of gradient around -1.2 is approached, in reasonable agreement with the value $-(\alpha + \beta + 1) = -1.4$ predicted by asymptotics. Similarly, an indication of the validity of (3.11) is provided by figure 6 where the gradient in the relevant regime is approximately -1.4; the value given by the asymptotic result $-(\alpha + \beta + 3)/2$ is -1.7, so the agreement is fair, the numerical results seeming to consistently overestimate the gradient somewhat.

In the gelating regime $\alpha + \beta > 1$, only the 'inner' region is present, numerical illustrations being given in [4]. We note from (3.7) that $q \to 0$ as $\omega \to -2$, suggesting that the inner and intermediate regions will merge; we shall now see that this is indeed the case. Similarly, as $\omega \to -1$ we have $n \to q$ and the intermediate and outer regions merge to give the two-region structure discussed in section 3.2.

3.4. The case $\omega < -2$

With $\omega < -2$, the input of monomers at large times is so slow that the large-time asymptotic structure of the solution is identical to that of the constant mass case studied earlier (see section 3 of [5]). To summarize this, for $j = \mathrm{O}(1)$, there is an inner solution of the separable form

$$c_j(t) \sim f_j/t \qquad \text{as} \quad t \to \infty. \tag{3.23}$$

For gelating cases this solution is uniformly valid and $f_j \sim Aj^{-(\alpha+\beta+3)/2}$ as $j \to \infty$ for some constant A. In non-gelating cases the solution (3.23) is not uniformly valid and an

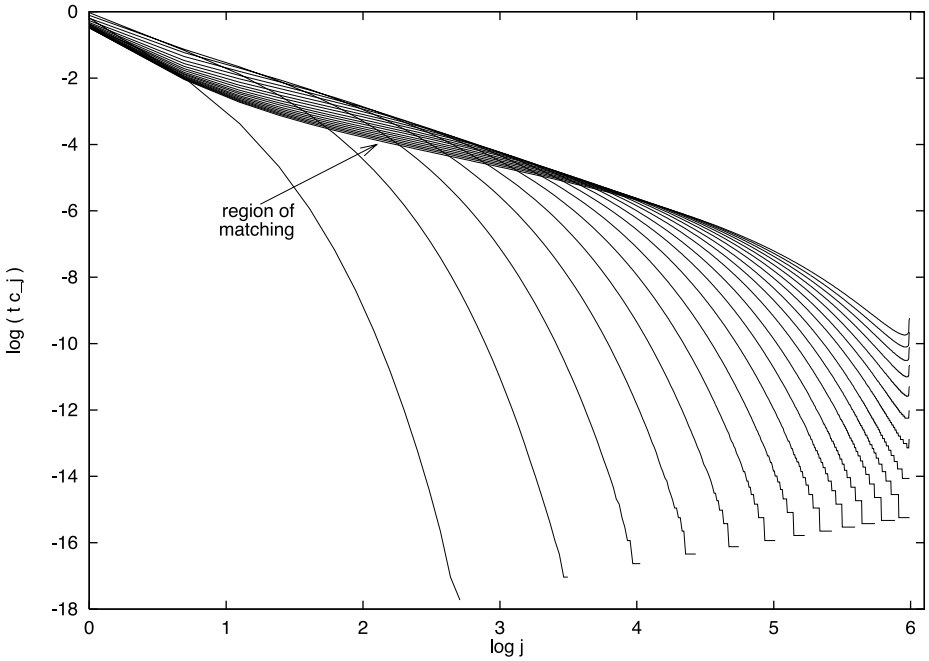

Figure 9. Plot of $\log(tc_j)$ against $\log j$ showing the inner solution at times $t = 0.2$–4, in steps of 0.2, for $\omega = -2.5$ and $\alpha = 0.3$, $\beta = 0.1$. At small j, the quantity $\log(tc_j)$ decreases with increasing time.

outer solution which exhibits a more rapid decay at large $j \equiv x$ is required (in particular, to avoid divergences in the density). This outer solution satisfies the continuum limit (3.1) of the coagulation equations, having the self-similar form (3.17), (3.19) and satisfying the conservation of mass conditions (3.18), (3.20). Matching the inner (3.23) and outer (3.17) solutions requires, in view of (3.22), that

$$f_j \sim \frac{2\alpha\beta j^{-(\alpha+\beta+1)}}{(1-(\alpha+\beta))(\alpha+\beta)B(1-\alpha,1-\beta)} \qquad \text{as} \quad j \to \infty. \tag{3.24}$$

These results are illustrated in figures 9 and 10 for $\alpha = 0.3$ and $\beta = 0.1$. Figure 10 gives plots of $\log(c_j t^{\frac{2}{1-(\alpha+\beta)}})$ against $\log(jt^{-\frac{1}{1-(\alpha+\beta)}})$, showing the concentrations with large j approaching a single curve at large times. Figure 9 illustrates the inner solution (3.23), approaching a straight line with gradient -1.2 for large enough j, which may be compared with the value of -1.4 predicted by (3.24). In both figures, effects due to the truncation of the system are seen in the slight increase in concentrations at large cluster sizes.

For $\omega = -2$, we conjecture that the asymptotic structure is as just described, but the function f_j in (3.23) (which is independent of ω for $\omega < -2$) differs because a full balance occurs in (1.1), (1.2); the source term and the time derivatives are of the same order as $t \to \infty$ (namely $O(t^{-2})$) in the critical case $\omega = -2$.

3.5. Complete gelation ($\alpha - \beta > 1$)

When α and β lie in the complete gelation regime, the infinite system (1.1), (1.2) has no solution; however, for the truncated system (3.3) a solution does exist and can be readily found numerically, providing insight into the non-existence of solutions to the infinite system.

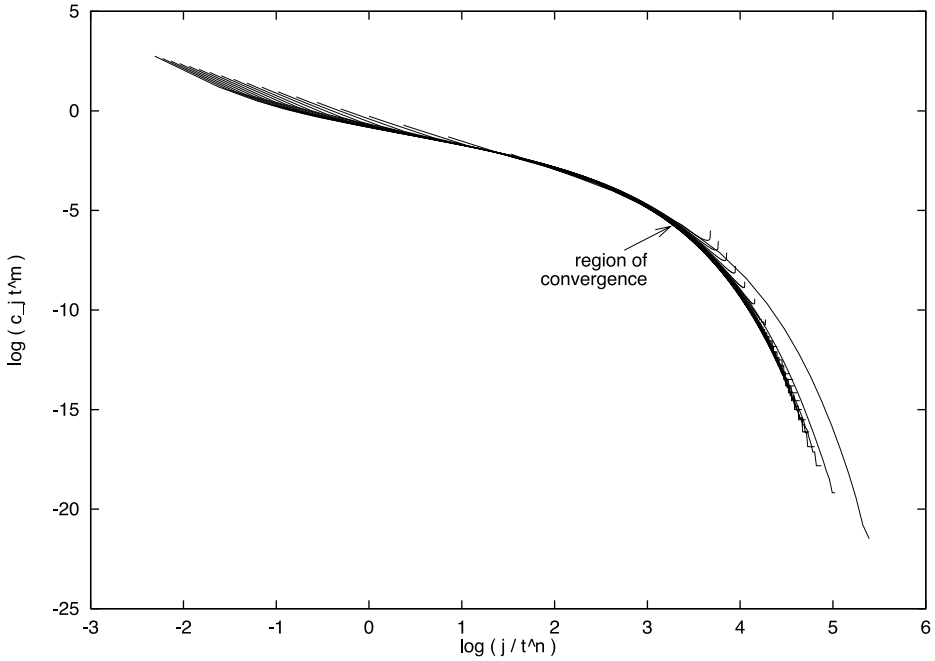

Figure 10. Plot of $\log(c_j t^m)$ against $\log(j/t^n)$ with $m = \frac{10}{3}$ and $n = \frac{5}{3}$ showing the outer solution (3.21) at times $t = 0.2$–4, in steps of 0.2, for $\omega = -2.5$ and $\alpha = 0.3$, $\beta = 0.1$.

Figure 11 shows that even at small times, the majority of the system's mass is in the largest cluster size. Monomers rapidly coagulate to form dimers, leading to a preponderance of dimers over monomers and a consequent domination of the system by clusters of even aggregation number. The resulting oscillatory profile is evident in figure 11. The mass of the gel (which we here define to be Nc_N) and the total mass of the system are plotted in figure 12. The gel rapidly takes up nearly the entire mass; this substantiates our assumption of complete gelation in the infinite system, whereby all the mass is in the form of gel, with $c_j = 0$ for finite j.

3.6. Summary

For $\alpha \geqslant \beta \geqslant 0$, the following regimes arise in the description of the large-time behaviour (we shall not discuss the borderline cases here).

(i) Complete gelation $\alpha - \beta > 1$. All the mass resides in the infinite gel particle.

(ii) Incomplete gelation $\alpha - \beta < 1$, $\alpha + \beta > 1$. Gelation occurs (either instantaneously ($\alpha > 1$) or after some finite time ($\alpha < 1$)) but the mass is not all transferred into the gel in finite time. We have

$$c_j(t) \sim t^{-1} f_j \qquad \text{as} \quad t \to \infty \qquad \omega < -2 \tag{3.25}$$

$$c_j(t) \sim t^{\omega/2} g_j \qquad \text{as} \quad t \to \infty \qquad \omega > -2 \tag{3.26}$$

for all j, with (3.25) satisfying the full system (1.1), (1.2), except that the source term is negligible, and with (3.26) satisfying the quasi-steady version of (1.1), (1.2), in which the left-hand sides are negligible. The f_j and g_j are each independent of ω.

(iii) No gelation $\alpha + \beta < 1$. The large-time forms (3.25), (3.26) remain valid for $j = \mathrm{O}(1)$,

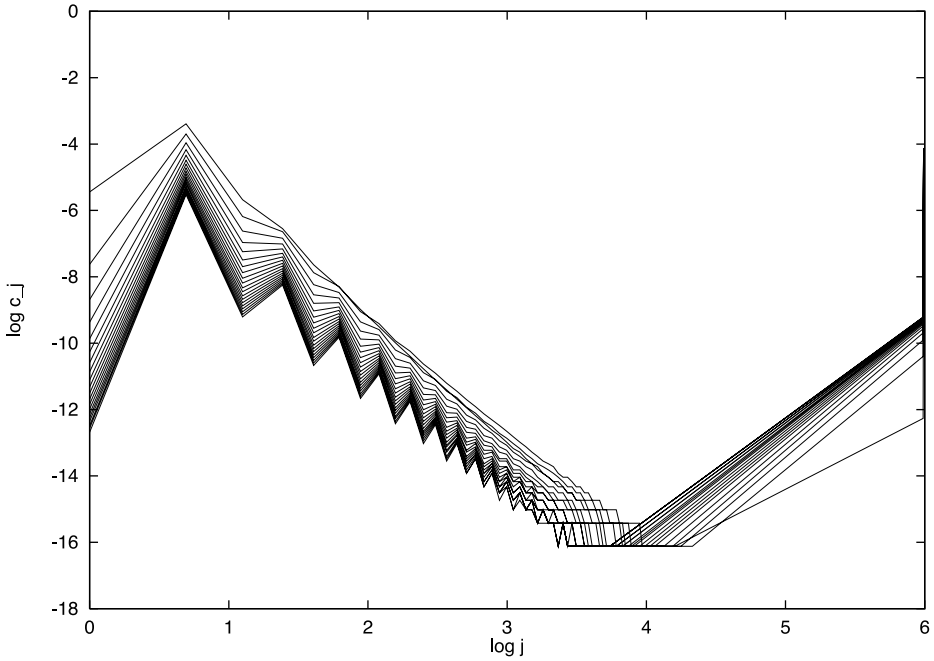

Figure 11. Plot of the numerical solution $\log c_j$ against $\log j$ for $\omega = -1.8$ and $\alpha = 2.5$, $\beta = 1.0$, at times $t = 0.2$–4 in steps of 0.2. The concentrations decrease with time for sufficiently small $\log j$ but increase for large $\log j$.

but different expressions hold for large j, specifically

$$c_j(t) \sim t^{-\frac{2}{1-(\alpha+\beta)}} g(j/t^{\frac{1}{1-(\alpha+\beta)}}) \qquad \text{as} \quad t \to \infty \quad \text{with} \quad j = \mathrm{O}(t^{\frac{1}{1-(\alpha+\beta)}}) \qquad \omega < -2 \tag{3.27}$$

$$c_j(t) \sim \begin{cases} t^{-p} h(j/t^q) & \text{as} \quad t \to \infty \quad \text{with} \quad j = \mathrm{O}(t^q) \\ t^{-\frac{2}{1-(\alpha+\beta)}} g(j/t^{\frac{1}{1-(\alpha+\beta)}}) & \text{as} \quad t \to \infty \quad \text{with} \quad j = \mathrm{O}(t^{\frac{1}{1-(\alpha+\beta)}}) \end{cases} \qquad -2 < \omega < -1 \tag{3.28}$$

$$c_j(t) \sim t^{-p} h(j/t^q) \qquad \text{as} \quad t \to \infty \quad \text{with} \quad j = \mathrm{O}(t^q) \qquad -1 < \omega \tag{3.29}$$

where p and q are given by (3.7) (implying $0 < q < 1$ for $-2 < \omega < -1$). Matching dictates that

$$h(\zeta) \sim A\zeta^{-(\alpha+\beta+3)/2} \qquad \text{as} \quad \zeta \to 0^+ \tag{3.30}$$

$$g(\eta) \sim \frac{2\alpha\beta\eta^{-(\alpha+\beta+1)}}{(1-(\alpha+\beta))(\alpha+\beta)B(1-\alpha, 1-\beta)} \qquad \text{as} \quad \eta \to 0^+ \tag{3.31}$$

so the two similarity solutions can be characterized by the distinct power laws which describe their local behaviour. For given α and β, the function $g(\eta)$ (which is independent of ω) is the same in (3.28) as it is in (3.29), with $g(\eta)$ decaying exponentially as $\eta \to \infty$; the same function $g(\eta)$ also arises in the constant mass case (see [5]). However, in (3.28) we have

$$h(\zeta) \sim \frac{2\alpha\beta\zeta^{-(\alpha+\beta+1)}}{(1-(\alpha+\beta))(\alpha+\beta)B(1-\alpha, 1-\beta)} \qquad \text{as} \quad \zeta \to +\infty \tag{3.32}$$

thereby matching with (3.31), whereas $h(\zeta)$ is exponentially decaying as $\zeta \to +\infty$ in (3.29).

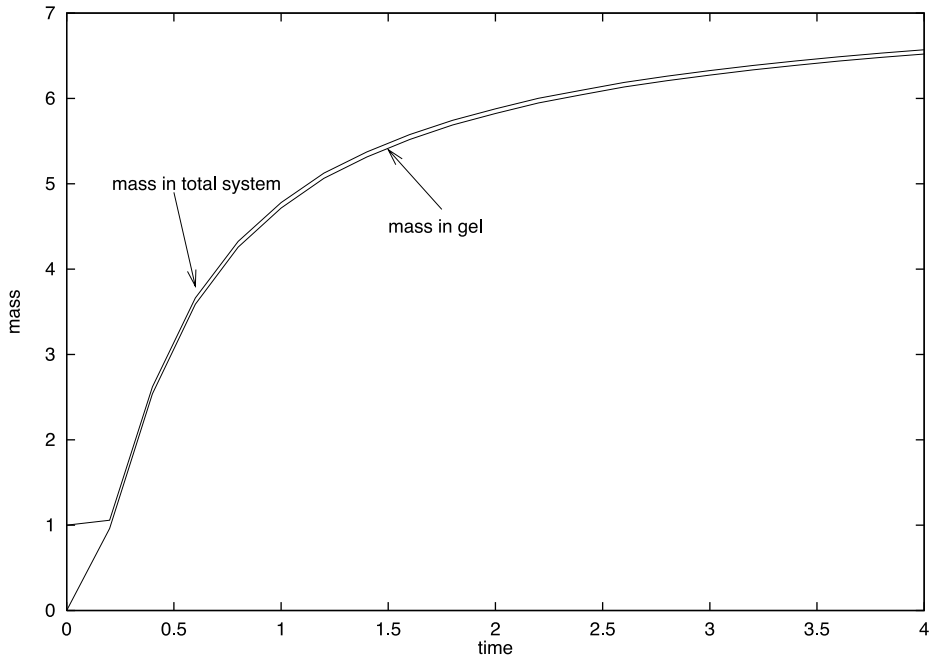

Figure 12. Plot of the amount of mass in the total system and the amount of mass within the gel for $\omega = -1.8$ and $\alpha = 2.5$, $\beta = 1.0$.

4. Discussion

In this paper we have used a combination of analytical, numerical and asymptotic methods to investigate the coagulation equations with an input term which is dependent on time. Our choice of injection rates includes (as the special case $\omega = 0$) mass being introduced at a constant rate. The 'integrable' systems, where α and β equal zero or one, do not appear to be solvable completely by analytical means, but the zeroth, first and second moments have been found exactly. For $\alpha = \beta = 1$ and $-1 < \omega$ the calculation of the second moment enables, in particular, the gelation time to be found.

For arbitrary positive α and β, the large-time asymptotics have been investigated. Such large-time results are applicable to more general injection rates whereby $Q_1(t) \sim t^{\omega}$ as $t \to \infty$ with $Q_j(t)$ decaying sufficiently rapidly for $j \geqslant 2$. A single regime is in force for all cluster sizes in the post-gelation phase of the reaction, with a more complex asymptotic structure present in systems which do not gelate. In the latter systems, there are three regions present for $-2 < \omega < -1$, two for $\omega > -1$ and two for $\omega < -2$. In this last case, mass is added so slowly that for large time the system behaves identically to the constant mass case studied earlier [5].

In systems which do not gelate, the large-time behaviour of the mass ($M_1(t)$) is simply the sum of the initial mass and the mass added, as given by (3.2). Mass is input in the form of monomers, so it is interesting to note the behaviour of the monomer concentration; in cases where $\omega > -2$, this is governed for large time by an inner quasi-steady state solution in which $c_1(t) \sim t^{\omega/2} g_1$, whereas in cases where $\omega < -2$ the inner solution has the similarity form $c_j(t) \sim f_j/t$.

Also worthy of note is the behaviour of the number of clusters ($M_0(t)$), the mass ($M_1(t)$)

and the second moment of the cluster distribution function ($M_2(t)$), for systems which do not gelate. For $\omega > -1$,

$$M_0(t) \sim \sum_{j=1}^{\infty} g_j t^{\omega/2} \qquad M_1(t) \sim \frac{t^{\omega+1}}{\omega+1} \qquad M_2(t) \sim \int_0^{\infty} \zeta^2 h(\zeta)\,\mathrm{d}\zeta\, t^{\omega+1+\frac{\omega+2}{1-(\alpha+\beta)}}$$
$$\text{as} \quad t \to \infty \tag{4.1}$$

the function $h(\zeta)$ being given by (3.9); M_0 is dominated by the inner region and M_1 and M_2 by the outer. The polydispersity ($M_2 M_0 / M_1^2$) thus scales with $t^{\frac{(\omega+2)(1+\alpha+\beta)}{2(1-(\alpha+\beta))}}$ in the large-time limit. For $-2 < \omega < -1$, the situation is a little more complicated since in the large-time asymptotics there are three size scales of significance, with the inner region dominating M_0 and the outer M_1 and M_2, with

$$M_0(t) \sim \sum_{j=1}^{\infty} g_j t^{\omega/2} \qquad M_1(t) \sim \varrho_0 - \frac{t_0^{\omega+1}}{\omega+1} \qquad M_2(t) \sim \int_0^{\infty} \eta^2 g(\eta)\,\mathrm{d}\eta\, t^{\frac{1}{1-(\alpha+\beta)}}$$
$$\text{as} \quad t \to \infty. \tag{4.2}$$

In this case the polydispersity increases without bound, scaling with $t^{\frac{\omega}{2}+\frac{1}{1-(\alpha+\beta)}}$ as $t \to \infty$. For $\omega < -2$, only the expression for M_0 changes in (4.2), giving

$$M_0(t) \sim \sum_{j=1}^{\infty} f_j t^{-1} \qquad M_1(t) \sim \varrho_0 - \frac{t_0^{\omega+1}}{\omega+1} \qquad M_2(t) \sim \int_0^{\infty} \eta^2 g(\eta)\,\mathrm{d}\eta\, t^{\frac{1}{1-(\alpha+\beta)}}$$
$$\text{as} \quad t \to \infty. \tag{4.3}$$

The polydispersity thus scales with $t^{\frac{\alpha+\beta}{1-(\alpha+\beta)}}$ as $t \to \infty$. In these systems we have coagulation and monomer addition occurring simultaneously, both causing the cluster distribution function to change. In all cases the polydispersity increases without bound; it is natural to conjecture that polydispersity is an increasing function of time in such systems. The results of section 2.1 are consistent with those just noted; the case $\alpha = 1$, $\beta = 0$ is non-generic (as noted in [5]), so the results of section 2.2 are not embodied in (4.1)–(4.3), which require $\alpha + \beta < 1$.

For each regime the numerical results have been shown to substantiate the asymptotics. If the parameters of the aggregation kernel allow gelation, then after gelation there is only one asymptotic region present, whatever the value of ω. A numerical solution for the truncated system in the complete gelation regime has been included; this shows that the gel (the largest cluster) very rapidly absorbs the vast majority of the mass, corresponding to the infinite system (1.1), (1.2) having no solution.

Acknowledgments

Both SCD and JADW wish to thank the University of Nottingham, SCD for a research studentship and JADW for the provision of computing equipment. JRK gratefully acknowledges the support of the Leverhulme Trust. We are grateful to Dr Iain Stewart for helpful discussions.

References

[1] Ball J M and Carr J 1990 The discrete coagulation-fragmentation equations: existence, uniqueness, and density conservation *J. Stat. Phys.* **61** 203–34

[2] Carr J and da Costa F P 1992 Instantaneous gelation in coagulation dynamics *Z. Angew. Math. Phys.* **43** 974–83

[3] Crump J G and Seinfeld J H 1982 On existence of steady-state solutions to the coagulation equations *J. Colloid Interface Sci.* **90** 469–76

[4] Davies S C 1998 *PhD Thesis* University of Nottingham
[5] Davies S C, King J R and Wattis J A D 1999 Self-similar behaviour in the coagulation equations *J. Eng. Math.* **36** 57–88
[6] van Dongen P G J and Ernst M H 1985 Cluster size distribution in irreversible aggregation at large times *J. Phys. A: Math. Gen.* **18** 2779–93
[7] van Dongen P G J 1987 Solutions of Smoluchowski's coagulation equation at large cluster sizes *Physica* A **145** 15–66
[8] van Dongen P G J 1987 On the possible occurrence of instantaneous gelation in Smoluchowski's coagulation equation *J. Phys. A: Math. Gen.* **20** 1889–904
[9] Hendriks E M 1984 Exact solution of a coagulation equation with removal term *J. Phys. A: Math. Gen.* **17** 2299–303
[10] Hendricks E M, Ernst M H and Ziff R M 1983 Coagulation equations with gelation *J. Stat. Phys.* **31** 519–63
[11] Hidy G M and Brock J R 1972 Topics in current aerosol research *International Reviews in Aerosol Physics and Chemistry* vol 2 (Oxford: Pergamon)
[12] Kleet J D 1975 A class of solutions to the steady-state, source-enhanced kinetic coagulation equation *J. Atmos. Sci.* **32** 380
[13] Leyvraz F and Tschudi H R 1981 Singularities in the kinetics of coagulation processes *J. Phys. A: Math. Gen.* **14** 3389–403
[14] Leyvraz F 1984 Large-time behaviour of the Smoluchowski equations of coagulation *Phys. Rev.* A **29** 854–8
[15] Lushnikov A A and Kulmala M 1995 Source-enhanced condensation in monocomponent disperse systems *Phys. Rev.* E **52** 1658–68
[16] Marques C M, Turner M S and Cates M E 1994 Relaxation mechanisms in worm-like micelles *J. Non-Cryst. Solids* **172–174** 1168–72
[17] Samsel R W and Perelson A S 1982 Kinetics of rouleau formation *Biophys. J.* **37** 493–514
[18] Simons S 1998 On the solution of the coagulation equations with a time-dependent source-application to pulsed injection *J. Phys. A: Math. Gen.* **31** 3759–68
[19] Singh P and Rodgers G R 1996 Coagulation processes with mass loss *J. Phys. A: Math. Gen.* **29** 437–50
[20] von Smoluchowski M 1916 Drei vorträge über diffusion Brownsche molekular bewegung und koagulation von kolloidteichen *Z. Phys.* **17** 557
[21] Wattis J A D and Coveney P V 1997 Generalized nucleation theory with inhibition for chemically reacting systems *J. Chem. Phys.* **106** 9122–40
[22] White W H 1982 On the form of steady-state solutions to the coagulation equations *J. Colloid Interface Sci.* **87** 204–8
[23] Ziff R M, Hendricks E M and Ernst M H 1982 Critical properties for gelation: a kinetic approach *Phys. Rev. Lett.* **49** 593–5